

Conjugated Polymers Based on a New Building Block: Dithienophthalimide

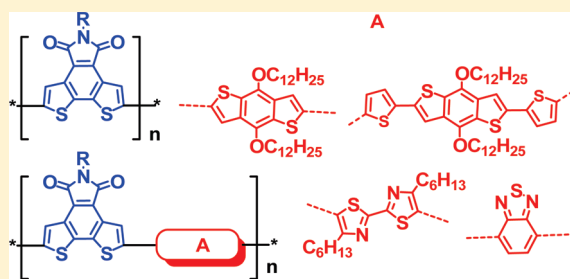
Haifeng Wang,^{†,‡} Qinqin Shi,^{†,‡} Yuze Lin,^{†,‡} Haijun Fan,^{†,‡} Pei Cheng,^{†,‡} Xiaowei Zhan,^{*,†} Yongfang Li,[†] and Daoben Zhu[†]

[†]Beijing National Laboratory for Molecular Sciences and Institute of Chemistry, Chinese Academy of Sciences, Beijing 100190, China

[‡]Graduate University of Chinese Academy of Sciences, Beijing 100049, China

 Supporting Information

ABSTRACT: A new fused-ring building block dithieno[3,2-*f*:2',3'-*h*]phthalimide was synthesized and used in synthesis of conjugated polymers. On the basis of this building block, we designed and synthesized a series of conjugated copolymers containing electron-rich unit benzo[1,2-*b*:4,5-*b'*]dithiophene (P1 and P2) or with electron-deficient unit 2,2'-bithiazole (P3 and P4) or benzo[*c*][1,2,5]thiadiazole (P5) and homopolymer (P6). P1 and P4–P6 have good solubility in common organic solvents, while P2 and P3 have poor solubility. P1–P6 exhibit good thermal stability with 5% weight loss temperatures of 193–417 °C. P1–P6 in films exhibit absorption maxima of 482–532 nm with optical bandgaps of 1.88–2.25 eV and weak emission peaked at 597–721 nm. P1–P6 have estimated HOMOs of –5.3 to –6.2 eV and LUMOs of –2.8 to –3.4 eV. The optical properties and HOMO/LUMO levels are influenced by the comonomers. The polymer solar cells based on P1:PC₆₁BM (1:1, w/w) exhibit preliminary power conversion efficiency of 0.30% under an AM 1.5 simulated solar light at 100 mW/cm².



INTRODUCTION

Significant progress has been made in synthesis of conjugated polymers and their applications for optoelectronic device such as organic light-emitting diodes (OLEDs), organic photovoltaic cells (OPVs), and organic field-effect transistors (OFETs) since Heeger, MacDiarmid, and Shirakawa discovered conducting polymers in 1976.¹ As a result of the low-cost, light-weight, and flexibility advantages, optoelectronic devices based on conjugated polymers are a promising cost-effective alternative to inorganic materials-based microelectronics. Conjugated polymers can be classified as hole (p-type) or electron (n-type) transporting materials according to the type of orderly transferring charge carriers. Most of conjugated polymers are p-type semiconductors that have seen a dramatic rise in performance over the past decade while much less attention has been devoted to n-type semiconducting polymers that have lagged behind their p-type counterparts.² Organic n-type materials are essential for the fabrication of organic p–n junctions, OPVs, n-channel OFETs, OLEDs, and complementary logic circuits.³

The n-type building blocks are the core components in n-type semiconducting polymers. Aromatic imides such as rylene diimides are one of the classical n-type building blocks and can exhibit relatively high electron affinities, high electron mobilities, and excellent chemical, thermal, and photochemical stabilities.⁴ These materials are electron deficient due to the substitution of an aromatic core with one or two sets of π -accepting imide groups that are mutually conjugated. The widely used rylene

diimides include perylene diimides (PDIs, 1) and naphthalene diimides (NDIs, 2) (Figure 1). Zhan and co-workers reported the synthesis of the first soluble rylene-based fully conjugated polymer.⁵ Top-gate OFETs based on this PDI–dithienothiophene copolymer exhibited a saturation electron mobility (μ_e) of $6 \times 10^{-2} \text{ cm}^2 \text{ V}^{-1} \text{ s}^{-1}$, current on/off ratio ($I_{\text{on}}/I_{\text{off}}$) of 10^4 , and a low threshold voltage (V_{th}) of 7 V in air.⁶ Moreover, all-polymer solar cells based on blends of polythiophene derivative donors and PDI–dithienothiophene copolymer acceptors exhibited power conversion efficiencies (PCEs) as high as 1.5% (AM1.5, 100 mW cm^{−2}).^{7–9} Facchetti et al. reported a conjugated copolymer of NDI and bithiophene;¹⁰ OFET devices based on this polymer fabricated in a top-gate, bottom-contact configuration with polymeric dielectrics exhibited μ_e of $0.1\text{--}0.85 \text{ cm}^2 \text{ V}^{-1} \text{ s}^{-1}$ under ambient conditions with $I_{\text{on}}/I_{\text{off}} > 10^5$.¹¹

The simplest aromatic imide system is phthalimide (3) and thiophene imide (4) (Figure 1). A few literatures reported phthalimide-containing conjugated polymers such as poly(phenylene ethynylene)s,¹² a polyaniline derivative,¹³ and a polythiophene derivative.¹⁴ In particular, Guo et al. reported that OFETs based on a phthalimide-containing polythiophene exhibited hole mobilities of $\sim 0.2 \text{ cm}^2 \text{ V}^{-1} \text{ s}^{-1}$ under ambient

Received: February 9, 2011

Revised: May 2, 2011

Published: May 16, 2011

conditions without optimization.¹⁴ Thiophene imide has simple, compact, symmetric, and planar structure. It could promote intrachain and interchain interactions along and between coplanar polymer chains. Zhang et al. pioneered to use thiophene imide as a building block in conjugated polymers.^{15,16} Later, thiophene imide homopolymers were synthesized.^{17–19} Recently, polymer solar cells based on blends of copolymers of thiophene imide and benzodithiophene^{20–23} or cyclopentadithiophene²⁴ with soluble fullerene derivatives PC₇₁BM or PC₆₁BM exhibited PCEs of 3–6.8%. Wudl et al. reported low-bandgap conjugated polymers based on thiophene-fused phthalimide, i.e., isothianaphthene imides (5, Figure 1).^{25,26} 2,2'-Bithiophene-3,3'-dicarboximide (BTI, 6, Figure 1) with π -core planarity, antiparallel BTI packing, a short cofacial π - π distance of 3.43 Å, and a favorable solubilizing group orientation is a promising building block in n-type polymers.²⁷ Facchetti et al. reported that n-channel OFET based on a bithiophene imide homopolymer exhibited a μ_e of $1.1 \times 10^{-2} \text{ cm}^2 \text{ V}^{-1} \text{ s}^{-1}$, $I_{\text{on}}/I_{\text{off}}$ of 2×10^7 , and a high V_{th} (75 V) in vacuum after annealing process at 240 °C.²⁷

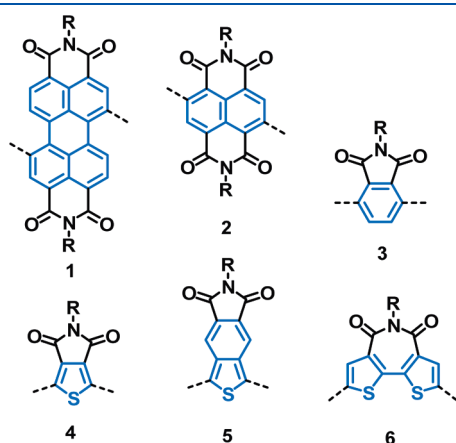


Figure 1. Some aromatic imide building blocks in conjugated polymers.

The fused-ring system can maximize the π -orbital overlap by restricting intramolecular rotation in the oligomer and possibly to induce face-to-face π -stacking, facilitating charge transport through intermolecular hopping. On the other hand, the fused rings can make the polymer backbone more rigid and coplanar, therefore enhancing effective π -conjugation, lowering bandgap, and extending absorption.^{28–31} Therefore, fused-ring building blocks are widely used in synthesis of conjugated polymers.^{32–34} For example, the large planar benzodithiophene (BDT) unit has emerged as an attractive building block for conjugated polymers.³⁵ Benzo[2,1-*b*:3,4-*b'*]dithiophene (7, Figure 2) with a curved structure prevents a fully conjugated pathway between substituents at the 2- and 6-positions. Hence, delocalization of the conjugated π -electron system along the copolymer backbone is disfavored by the incorporation of this unit. This increases the ionization potential of the polymer and is thus expected to improve air stability under operation. Additionally, compared to a single thiophene ring, it must be pointed out that due to the large resonance stabilization energy of BDT, the delocalization of electrons from the BDT unit into the backbone is less favorable than from the thiophene ring. As a result, a more stable copolymer with high performance can be obtained by using BDT as the core unit. OFETs based on a benzo[2,1-*b*:3,4-*b'*]dithiophene copolymer manufactured on flexible substrate exhibited high hole mobility of $0.5 \text{ cm}^2 \text{ V}^{-1} \text{ s}^{-1}$ when the source-gate voltage is increased to 60 V.³⁶ OPVs based on blends of benzo[2,1-*b*:3,4-*b'*]dithiophene copolymers and PC₆₁BM exhibited PCEs as high as 2.17%.^{37–40}

In this paper, we report creation of a new fused-ring building block dithieno[3,2-*f*:2',3'-*h'*]phthalimide (8, Figure 2) and its application in design and synthesis of conjugated polymers. The combination of benzo[2,1-*b*:3,4-*b'*]dithiophene planarity and efficient π - π stacking with the electron-withdrawing capacity of the imide functionality serves as the foundation for this new class of materials. Introduction of the π -electron-deficient imide moiety can decrease the HOMO and LUMO energies of the polymers, which is necessary for air-stable polymers.

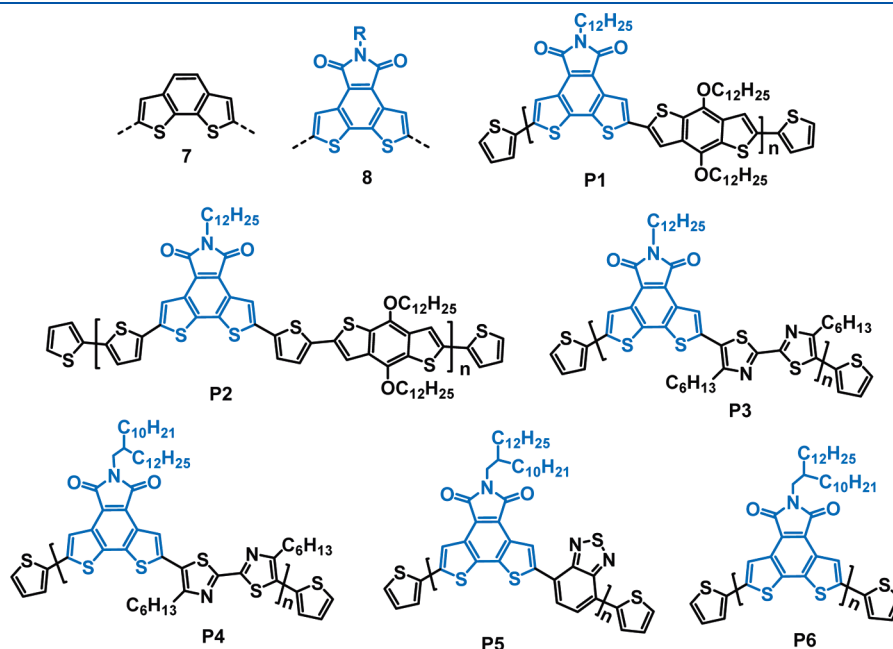
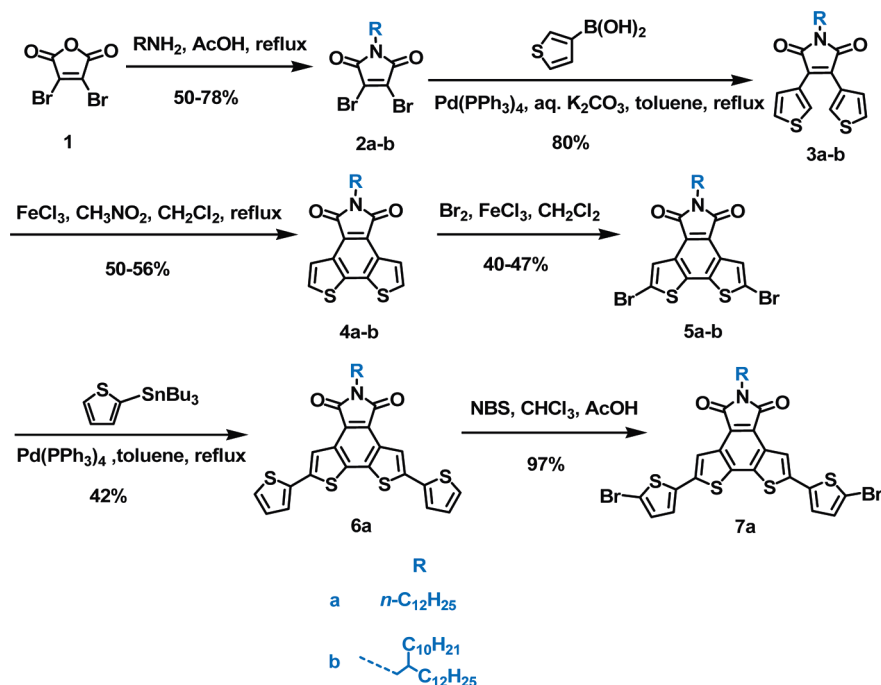


Figure 2. Chemical structures of conjugated polymers based on dithieno[3,2-*f*:2',3'-*h'*]phthalimide.

Scheme 1. Synthesis of the Monomers



Furthermore, substitution at the imide nitrogen allows introduction of functionalities and solubility improvement with varying degrees of steric bulk while not impinging on critical intermolecular π – π stacking characteristics. This motif also leaves the benzo[2,1-*b*:3,4-*b'*]dithiophene 2- and 7-positions available for polymerization. Finally, the dipole moment caused by the imide could stabilize cofacial antiparallel intra- and interchain repeat unit orientations, planarize the backbone, and promote π – π stacking.²⁷ On the basis of this new building block, we designed and synthesized a series of conjugated copolymers: unit **8** coupled with electron-rich unit benzo[1,2-*b*:4,5-*b'*]dithiophene (**P1** and **P2**) or with electron-deficient unit 2,2'-bithiazole (**P3** and **P4**) or benzo[*c*][1,2,5]thiadiazole (**P5**) and homopolymer (**P6**) (Figure 2). The optical properties and electronic structure (HOMO/LUMO levels and bandgap) can be manipulated through adjusting copolymerized building blocks.

RESULTS AND DISCUSSION

Synthesis and Characterization. The synthetic routes to the monomers and polymers are outlined in Schemes 1 and 2. We chose very cheap, industrial product maleic anhydride as a starting material. Bromination of maleic anhydride with Br_2 gave its dibromide (**1**).⁴¹ Then, amination with alkylamine afforded the alkyl-substituted 3,4-dibromopyrrole-2,5-dione (**2a,b**). Suzuki coupling reaction of the dibromide **2a,b** with 3-thienylboronic acid gave 3,4-bis(3-thienyl)pyrrole-2,5-dione (**3a,b**). The large sulfur-containing polycyclic aromatic imides, dithieno[3,2-*f*:2',3'-*h'*]phthalimide (**4a,b**), were synthesized through iron(III) chloride-mediated oxidative cyclization, which is a general strategy for ring closure.⁴² Bromination of **4a,b** with Br_2 gave rise to the monomers **5a,b**. Stille coupling reaction of **5a** with tributyl(thiophen-2-yl)stannane afforded 2,7-bis(2-thienyl)-

dithieno[3,2-*f*:2',3'-*h'*]phthalimide (**6a**), which was brominated with NBS to afford monomer **7a**.

Copolymers **P1**–**P4** were synthesized through Stille reaction of the dibromide monomers **5a,b** or **7a** with benzo-dithiophene-2,6-ditin or 2,2'-bithiazole-5,5'-ditin, while **P5** was synthesized through Suzuki coupling reaction of the dibromide monomer **5b** with benzothiadiazole-4,7-diboronic ester. Homopolymer **P6** was synthesized by palladium-catalyzed homocoupling of the dibromide **5b** in the presence of hexabutyltin. **P1** with three solubilizing *n*-dodecyl groups has good solubility in common organic solvents such as chloroform, THF, and toluene. However, **P2** with thiophene spacer between two large units **8** and BDT has poor solubility due to more planar conformation and stronger interchain interactions caused by smaller torsion angle. To our surprise, **P3** with three solubilizing *n*-alkyl groups also has poor solubility probably due to strong interchain interactions. Replacing *n*-dodecyl in **P3** with 2-decyltetradecyl group significantly enhance solubility of **P4**. **P5** and **P6** also have good solubility.

Molecular weights of the polymers were determined by gel permeation chromatography (GPC) using polystyrene standards as calibrants. The polymers **P1** and **P4**–**P6** show number-average molecular weight (M_n) of 12 250, 9934, 5714, and 10 053, with polydispersity indices (M_w/M_n) of 1.30, 1.43, 1.71, and 1.56, respectively (Table 1). The GPC measurements for **P2** and **P3** are not carried out due to their low solubility. The thermal properties of the polymers were determined by thermogravimetric analysis (TGA) under nitrogen (Figure 2). The decomposition temperature (T_d) at 5% weight loss for **P3**–**P6** are above 330 °C, while **P1** and **P2** exhibit lower T_d (below 300 °C) (Table 1).

Optical Properties. The UV–vis absorption and photoluminescence (PL) spectra of **P1**–**P6** were measured in CHCl_3 (ca. 10^{-6} M) solution and in thin films, and the results are

Scheme 2. Synthesis of the Polymers

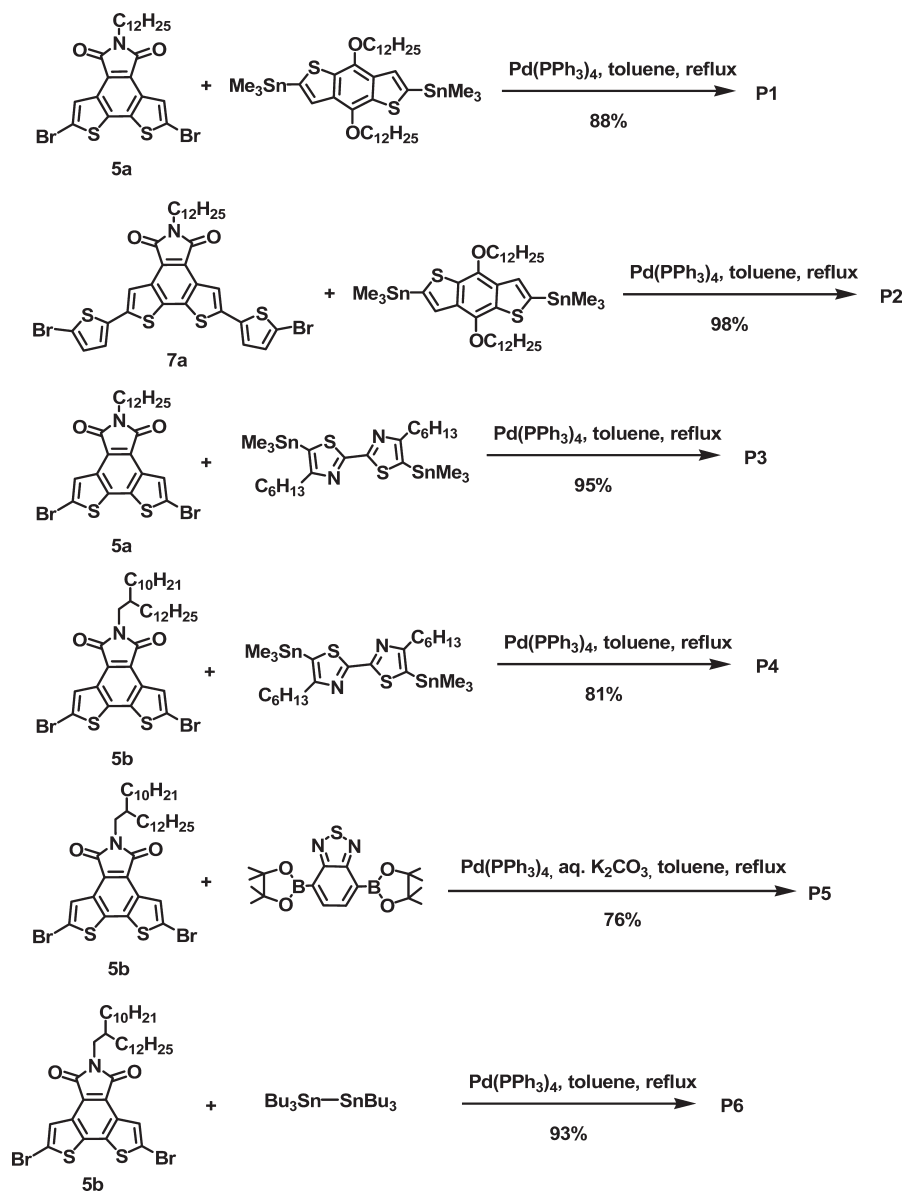


Table 1. Molecular Weights and Thermal Properties of the Polymers

	yield (%)	M_n^a	M_w^a	M_w/M_n^a	T_d^b (°C)
P1	88	12250	15950	1.30	270
P2 ^c	98				193
P3 ^c	95				417
P4	81	9934	14234	1.43	379
P5	76	5714	9784	1.71	338
P6	93	10053	15613	1.56	384

^aNumber-average molecular weight (M_n), weight-average molecular weight (M_w), and polydispersity index (M_w/M_n) determined by means of GPC with THF as eluent on the basis of polystyrene calibration. ^bTemperature at 5% weight loss estimated using TGA under N_2 . ^cAs a result of poor solubility, GPC measurements were not carried out.

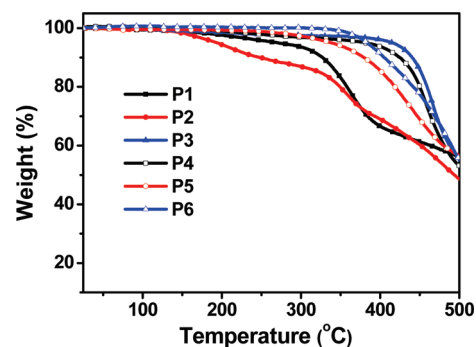


Figure 3. TGA curves of the polymers.

summarized in Table 2. Homopolymer P6 in solution and in film exhibits absorbance maxima at 464 and 482 nm, which are

Table 2. Absorption/PL Maxima and HOMO/LUMO Energy Levels of P1–P6 and 4b

	λ_{abs}^a (nm)		λ_{PL}^b (nm)		$E_{\text{g}}^{\text{opt c}}$ (eV)	HOMO ^d (eV)	LUMO ^d (eV)	$E_{\text{g}}^{\text{cv e}}$ (eV)
	solution	film	solution	film				
P1	496	500	661	636	2.11	−5.55	−2.78	2.77
P2	510	532	626		1.93	−5.33	−2.77	2.56
P3	484	506	636	669	2.08	−6.04	−3.04	3.00
P4	483	504	641	667	2.09	−6.02	−3.06	2.96
P5	503	524	672	721	1.88	−5.98	−3.38	2.60
P6	464	482	531	597	2.25	−6.20	−3.10	3.10
4b	376	370	453	508	2.97	−6.25	−3.12	3.13

^a Absorption maxima. ^b PL maxima. ^c Estimated from the onset edge of absorption in film. ^d Estimated from the onset oxidation and reduction potentials, respectively, assuming the absolute energy level of ferrocene/ferrocenium to be 4.8 eV below vacuum. ^e HOMO–LUMO gap estimated electrochemistry.

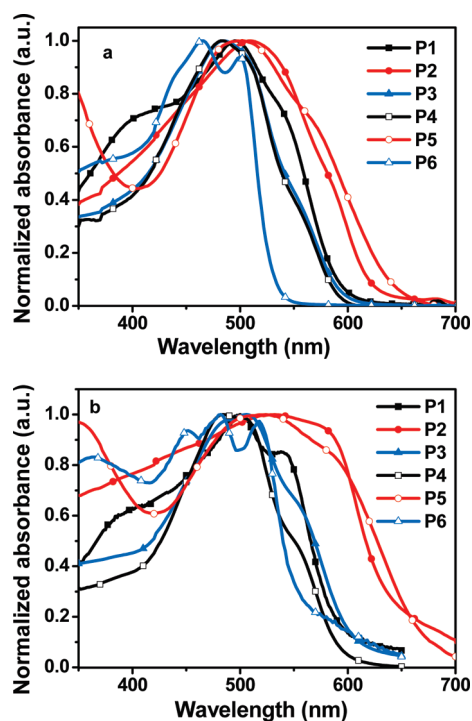


Figure 4. Absorption spectra of P1–P6 in CHCl₃ solution (a) and in thin film (b).

red-shifted 88 and 112 nm respectively, relative to monomer 4b (Figure S1, Supporting Information) due to increased conjugation. Compared to homopolymer P6, all copolymers P1–P5 exhibit red-shifted absorptions and smaller optical bandgaps in solution and in film. Broad absorption bands located in the visible region were observed for the solution and film of P1 (Figure 4). The absorbance maximum for P1 in solution is 496 nm. The absorption spectrum of P1 in film exhibits red-shift and distinct shoulder peak at ca. 540 nm, which are probably related to the formation of molecular aggregates owing to the strong interchain interactions. The absorption maxima of P2 in solution and in film are red-shifted 14 and 32 nm relative to that of P1, respectively, thanks to its more planar conformation and increased conjugation. P3 and P4 exhibit almost same absorption profile in solution and in film. Compared to P1 and P2, P3 and P4 exhibit relatively narrow and blue-shifted absorption band in solution

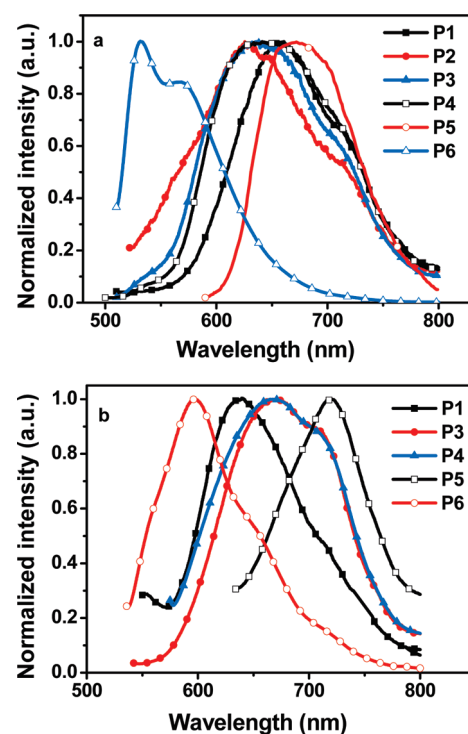


Figure 5. PL spectra of P1–P6 in CHCl₃ solution (a) and in thin film (b), no emission from P2 film.

and in film. P5 in solution and in film exhibits absorbance maxima at 503 and 524 nm, which are shifted 20 nm to the red relative to those of P4, suggesting a more planar conformation.

The trend in emission spectra of P1–P6 in solution and in film resembles that in their absorption spectra. The copolymers P1–P5 emit weak fluorescence both in solution and in film with very large Stokes shifts (120–200 nm) (Figure 5), suggesting that the polymers undergo considerable molecular rearrangement upon photoexcitation, leading to a big structural difference between the excited and ground states.^{43,44}

Electrochemical Properties. The redox behavior for P1–P6 and small molecule 4b were investigated by cyclic voltammetry (Figure 6). The monomer 4b shows a reversible reduction wave and an irreversible oxidation wave. The HOMO and LUMO levels were estimated from the onset oxidation and reduction potentials, assuming the absolute energy level of ferrocene/ferrocenium to

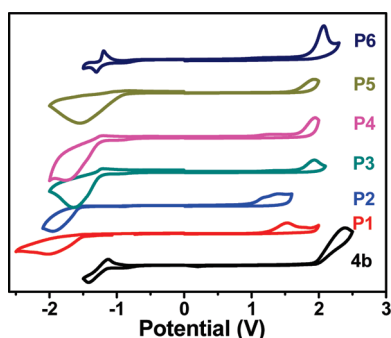


Figure 6. Cyclic voltammograms of **P1**–**P6** films in $\text{CH}_3\text{CN}/0.1 \text{ M } [\text{Bu}_4\text{N}]^+[\text{PF}_6]^-$ and **4b** in CH_2Cl_2 solution/ $0.1 \text{ M } [\text{Bu}_4\text{N}]^+[\text{PF}_6]^-$ at 50 mV s^{-1} . The horizontal scale potential is referenced to an anodized Ag wire pseudoreference electrode.

be 4.8 eV below vacuum, and the data are summarized in Table 2. The LUMO of **4b** is -3.12 eV , which is similar to that (ca. -3.23 eV) of n-type building block BTI (**6**, Figure 1).²⁷ As it is generally assumed that a high electron affinity ($>3 \text{ eV}$) is necessary for n-type materials,^{4,45,46} we suggest that dithieno[3,2-*f*:2',3'-*h*]phthalimide functions as a n-type building block. However, compared to the very strong n-type building blocks PDI (**1**, Figure 1) and NDI (**2**, Figure 1) (LUMO $\approx -3.8 \text{ eV}$),⁴ dithieno[3,2-*f*:2',3'-*h*]phthalimide is relatively a weak n-type building block. The homopolymer **P6** shows a reversible reduction wave and an irreversible oxidation wave. **P6** exhibits HOMO/LUMO levels of $-6.2/-3.1 \text{ eV}$, which is close to that of **4b**. Compared to benzo[2,1-*b*:3,4-*b'*]dithiophene homopolymers, which exhibited the HOMO/LUMO of $-5.7/-2.65 \text{ eV}$ ³⁸ or $-5.33/-2.57 \text{ eV}$,³⁹ the imide moiety indeed significantly lowers the HOMO/LUMO. However, the LUMO of **P6** is higher than that of BTI homopolymer (-3.47 eV).²⁷

Copolymers **P1**–**P5** exhibit an irreversible reduction peak and an irreversible oxidation peak. The HOMO/LUMO of **P1** is $-5.55/-2.78 \text{ eV}$; the electron-rich unit benzo[1,2-*b*:4,5-*b'*]dithiophene leads to upshifting of HOMO/LUMO levels compared to homopolymer **P6**. The LUMO of **P1** is higher than that of poly[thiopheneimide-*alt*-benzo[1,2-*b*:4,5-*b'*]dithiophene] (-3.6 eV),²⁰ indicating that the electron-withdrawing ability of dithieno[3,2-*f*:2',3'-*h*]phthalimide is weaker than that of thiophene imide (**4**, Figure 1). As a result of two more electron-donating thiophenes in the polymer backbone, the HOMO of **P2** increases by 0.22 eV relative to that of **P1**. **P3** and **P4** with weak electron-deficient unit 2,2'-bithiazole exhibit similar HOMO/LUMO levels to homopolymer **P6**, while the stronger electron-accepting unit benzo[*c*][1,2,5]thiadiazole reduced the LUMO by 0.28 eV . The HOMO–LUMO gaps E_g^{cv} , estimated from electrochemistry, are larger than the optical bandgaps E_g^{opt} , very similar to that for BTI homopolymer and copolymer.²⁷

Photovoltaic Cells. To demonstrate potential application of dithieno[3,2-*f*:2',3'-*h*]phthalimide-based polymers in organic photovoltaics (OPV), we chose **P1** as an example to fabricate polymer solar cell devices because it possesses relatively broad absorption, proper HOMO/LUMO energy levels, and good solubility. Using **P1** as electron donor and solution-processable fullerene derivative PC_{61}BM as electron acceptor, we fabricated bulk heterojunction OPV devices with a structure of ITO/PEDOT:PSS/**P1**: PC_{61}BM (1:1, w/w)/Al. Without any device optimization, the device afforded an open circuit voltage (V_{oc}) of

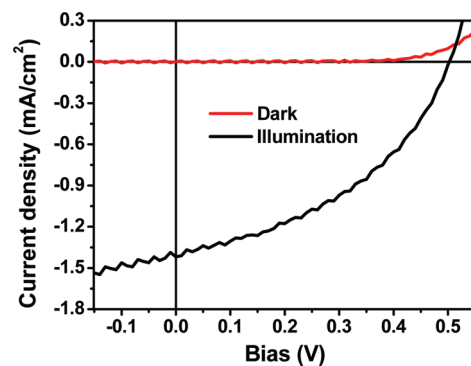


Figure 7. Current density–voltage characteristics of a device with the structure of ITO/PEDOT:PSS/**P1**: PC_{61}BM (1:1, w/w)/Al in dark as well as under illumination of AM1.5, 100 mW/cm^2 .

0.50 V , a short-circuit current density (J_{sc}) of 1.42 mA/cm^2 , a fill factor (FF) of 42.4% , and a preliminary power conversion efficiency (PCE) of 0.30% under an AM 1.5 simulated solar light at 100 mW/cm^2 (Figure 7). The PCE is lower than that of poly[thiopheneimide-*alt*-benzo[1,2-*b*:4,5-*b'*]dithiophene],^{20–22} probably due to low hole mobility of **P1** (ca. $10^{-6} \text{ cm}^2 \text{ V}^{-1} \text{ s}^{-1}$).

CONCLUSION

We have designed and synthesized a new fused-ring building block, dithieno[3,2-*f*:2',3'-*h*]phthalimide. On the basis of this new building block, we have designed and synthesized a series of new conjugated copolymers containing electron-rich unit benzo[dithiophene] or electron-deficient unit bithiazole or benzothiadiazole and homopolymers. The optical properties and HOMO/LUMO levels can be manipulated through adjusting copolymerized building blocks. Compared to homopolymer **P6**, all copolymers **P1**–**P5** exhibit red-shifted absorption and emission spectra in solution and in film and smaller bandgaps. Dithieno[3,2-*f*:2',3'-*h*]phthalimide and its homopolymer exhibit low HOMO of -6.2 eV and relatively low LUMO of -3.1 eV , indicating that it is relatively weak n-type building block. Increase in electron-donating strength of the counit leads to upshift in both HOMO and LUMO, while increase in electron-withdrawing strength of the counit leads to downshift in both HOMO and LUMO. Preliminary OPV results show that polymer solar cells based on **P1**: PC_{61}BM (1:1, w/w) gave a PCE of 0.30% under an AM 1.5 simulated solar light at 100 mW/cm^2 .

EXPERIMENTAL SECTION

Materials. Unless stated otherwise, starting materials were obtained from Aldrich or Acros and were used without further purification. THF and toluene were distilled from sodium benzophenone under nitrogen prior to use. 3,4-Dibromofuran-2,5-dione (**1**) was synthesized according to the literature method.⁴¹ 4,8-Didodecyloxybenzodithiophene-2,6-ditin and 4,4'-dihexyl-2,2'-bithiazole-5,5'-ditin were synthesized according to our published procedures.⁴⁷

Characterization. The ^1H and ^{13}C NMR spectra were measured on a Bruker AVANCE 400 spectrometer. Mass spectra were measured on a GCT-MS micromass spectrometer using EI mode or on a Bruker Daltonics BIFLEX III MALDI-TOF Analyzer using MALDI mode. Elemental analyses were carried out using a FLASH EA1112 elemental analyzer. Solution (chloroform) and thin-film (on quartz substrate) UV–vis absorption spectra were recorded on a JASCO V-570 spectrophotometer.

Solution (CHCl_3) and thin-film (on quartz substrate) emission spectra were collected on a Hitachi F-4500 spectrofluorophotometer. Electrochemical measurements for polymers **P1**–**P6** were carried out under nitrogen on a deoxygenated solution of tetra-*n*-butylammonium hexafluorophosphate (0.1 M) in CH_3CN using a computer-controlled Zahner IM6e electrochemical workstation, a glassy-carbon working electrode coated with polymer films, a platinum-wire auxiliary electrode, and an Ag wire anodized with AgCl as a pseudoreference electrode. Electrochemical measurements for small molecule **4b** were carried out under nitrogen on a deoxygenated solution of tetra-*n*-butylammonium hexafluorophosphate (0.1 M) in distilled CH_2Cl_2 using a computer-controlled Zahner IM6e electrochemical workstation, a glassy-carbon working electrode, a platinum-wire auxiliary electrode, and an Ag wire anodized with AgCl as a pseudoreference electrode. Thermogravimetric analysis (TGA) measurements were performed on Shimadzu thermogravimetric analyzer (model DTG-60) under a nitrogen flow at a heating rate of $10\text{ }^\circ\text{C min}^{-1}$.

Fabrication and Characterization of Polymer Solar Cells.

OPV devices were fabricated with a structure of ITO/PEDOT:PSS/**P1**:PC₆₁BM/Al. The patterned indium tin oxide (ITO) glass (sheet resistance $30\text{ }\Omega/\square$) was precleaned in an ultrasonic bath of acetone and isopropanol and treated in an ultraviolet-ozone chamber (Jelight Company) for 30 min. A thin layer (30 nm) of poly(3,4-ethylenedioxythiophene):poly(styrenesulfonate) (PEDOT:PSS, Baytron P VP A1 4083, Germany) was spin-coated onto the ITO glass and baked at $150\text{ }^\circ\text{C}$ for 30 min. A chlorobenzene solution of a blend of **P1**/PC₆₁BM (1:1, w/w) was subsequently spin-coated on the surface of the PEDOT:PSS layer to form a photosensitive layer. An aluminum layer (ca. 60 nm) was then evaporated onto the surface of the photosensitive layer under vacuum (ca. 10^{-4} Pa). The active area of the device was 4 mm^2 . The current voltage curve was measured with a computer-controlled Keithley 236 Source Measure Unit. A xenon lamp coupled with AM 1.5 solar spectrum filters was used as the light source, and the optical power at the sample was 100 mW/cm^2 .

Synthesis. *3,4-Dibromo-1-dodecylpyrrole-2,5-dione (2a)*. To a solution of 3,4-dibromomaleic anhydride (**1**) (2.56 g, 10 mmol) in acetic acid (25 mL) was added *n*-C₁₂H₂₅NH₂ (2.59 g, 14 mmol). After refluxing for 16 h, the mixture was cooled to room temperature, poured into saturated NaHCO₃ aqueous solution. The organic products were extracted by CH_2Cl_2 and dried over anhydrous MgSO₄. The crude product was purified by column chromatography on silica gel (CH_2Cl_2 /hexanes = 1:3) to give **2a** as a pale yellow solid (3.32 g, 78%). ¹H NMR (400 MHz, CDCl₃): δ 3.61 (t, *J* = 7.3 Hz, 2H), 1.61 (m, 2H), 1.27 (m, 18H), 0.89 (t, *J* = 6.7 Hz, 3H). ¹³C NMR (100 MHz, CDCl₃): δ 163.82, 129.24, 39.76, 31.89, 29.59, 29.53, 29.42, 29.32, 29.05, 28.40, 26.60, 22.67, 14.12. HRMS (EI): 421.0248 (calcd for C₁₆H₂₅NO₂Br₂, 421.0252). Anal. Calcd for C₁₆H₂₅NO₂Br₂: C, 45.41; H, 5.95; N, 3.31. Found: C, 45.33; H, 5.94; N, 3.09%.

3,4-Dibromo-1-(2-decyltetradecyl)pyrrole-2,5-dione (2b). The same procedure as **2a** using 2-decyltetradecylamine instead of *n*-C₁₂H₂₅NH₂ to give **2b** as a pale yellow semisolid (50%). ¹H NMR (400 MHz, CDCl₃): δ 3.49 (d, *J* = 7.1 Hz, 2H), 1.75 (m, 1H), 1.25 (m, 40H), 0.89 (t, *J* = 6.8 Hz, 6H). ¹³C NMR (100 MHz, CDCl₃): δ 164.15, 129.27, 43.93, 37.04, 31.99, 31.32, 29.94, 29.73, 29.69, 29.64, 29.42, 29.41, 26.22, 22.75, 14.17. HRMS (EI): 589.2124 (calcd for C₂₈H₄₉NO₂Br₂, 589.2130). Anal. Calcd for C₂₈H₄₉NO₂Br₂: C, 56.86; H, 8.35; N, 2.37. Found: C, 56.96; H, 8.14; N, 2.14%.

1-(2-Decyltetradecyl)-3,4-bis(thiophen-3-yl)pyrrole-2,5-dione (3a). To a mixture of **2a** (423 mg, 1 mmol), 3-thiopheneboronic acid (320 mg, 2.5 mmol), 2 M K₂CO₃ aqueous solution (2 mL), and toluene (4 mL) was added Pd(PPh₃)₄ (115 mg, 0.1 mmol) under a N₂ atmosphere. After refluxing for 48 h, the mixture was cooled to room temperature, then poured into H₂O. The organic layer was extracted by CH_2Cl_2 and dried over anhydrous MgSO₄. The crude product was purified by column chromatography on silica gel (CH_2Cl_2 /hexanes = 1:2) to give **3a** as a

yellow solid (345 mg, 80%). ¹H NMR (400 MHz, CD₂Cl₂): δ 7.98 (d, *J* = 2.1 Hz, 2H), 7.34 (dd, *J* = 4.9 Hz, 3.0 Hz, 2H), 7.25 (d, *J* = 5.1 Hz, 2H), 3.62 (t, *J* = 7.4 Hz, 2H), 1.66 (m, 2H), 1.25 (m, 18H), 0.88 (t, *J* = 6.8 Hz, 3H). ¹³C NMR (100 MHz, CD₂Cl₂): δ 171.03, 129.43, 129.07, 127.63, 125.74, 38.43, 31.94, 29.66, 29.62, 29.52, 29.38, 29.23, 28.62, 26.87, 22.72, 14.18. HRMS (EI): 429.1801 (calcd for C₂₄H₃₁NO₂S₂, 429.1796). Anal. Calcd for C₂₄H₃₁NO₂S₂: C, 67.09; H, 7.27; N, 3.26. Found: C, 67.04; H, 7.30; N, 3.24%.

1-(2-Decyltetradecyl)-3,4-bis(thiophen-3-yl)pyrrole-2,5-dione (3b).

The same procedure as **3a** using **2b** instead of **2a** to give **3b** as a yellow semisolid (80%). ¹H NMR (400 MHz, CD₂Cl₂): δ 7.99 (dd, *J* = 2.8 Hz, 0.7 Hz, 2H), 7.34 (dd, *J* = 5.1 Hz, 2.9 Hz, 2H), 7.27 (dd, *J* = 5.0 Hz, 0.7 Hz, 2H), 3.51 (d, *J* = 7.2 Hz, 2H), 1.75 (m, 1H), 1.25 (m, 40H), 0.89 (t, *J* = 6.5 Hz, 6H). ¹³C NMR (100 MHz, CD₂Cl₂): δ 171.32, 129.48, 129.05, 127.69, 125.74, 42.69, 37.10, 31.99, 31.57, 30.03, 29.76, 29.72, 29.68, 29.42, 26.39, 22.76, 14.19. MS (MALDI): *m/z* 598 (MH⁺). Anal. Calcd for C₃₆H₅₅NO₂S₂: C, 72.31; H, 9.27; N, 2.34. Found: C, 72.03; H, 9.20; N, 2.24%.

N-Dodecylthiophene[3,2-f:2',3'-h]phthalimide (4a).

To a solution of **3a** (214 mg, 0.5 mmol) in CH_2Cl_2 (300 mL) was added FeCl₃ (1.63 g, 10 mmol, dissolved in 10 mL of CH_3NO_2) under a N₂ atmosphere. After refluxing for 12 h, the reaction was quenched by adding CH₃OH (50 mL). The mixture was washed with saturated NaCl and NH₄Cl aqueous solution subsequently, and then the organic layer was dried over anhydrous MgSO₄. The crude product was purified by column chromatography on silica gel (CH_2Cl_2 /hexanes = 1:2) to give **4a** as a yellow solid (120 mg, 56%). ¹H NMR (400 MHz, CDCl₃): δ 8.09 (d, *J* = 5.0 Hz, 2H), 7.68 (d, *J* = 5.4 Hz, 2H), 3.75 (t, *J* = 7.2 Hz, 2H), 1.74 (m, 2H), 1.24 (m, 18H), 0.88 (t, *J* = 6.6 Hz, 3H). ¹³C NMR (100 MHz, CDCl₃): δ 168.86, 139.17, 130.54, 128.62, 123.43, 122.24, 37.96, 31.93, 29.65, 29.56, 29.37, 29.29, 28.88, 26.99, 22.71, 14.16. HRMS (EI): 427.1644 (calcd for C₂₄H₂₉NO₂S₂, 427.1640). Anal. Calcd for C₂₄H₂₉NO₂S₂: C, 67.41; H, 6.84; N, 3.28. Found: C, 67.20; H, 6.88; N, 3.56%.

N-(2-Decyltetradecyl)thiophene[3,2-f:2',3'-h]phthalimide (4b).

The same procedure as **4a** using **3b** instead of **3a** to give **4b** as a yellow solid (50%). ¹H NMR (400 MHz, CDCl₃): δ 8.11 (d, *J* = 5.2 Hz, 2H), 7.69 (d, *J* = 5.3 Hz, 2H), 3.63 (d, *J* = 7.2 Hz, 2H), 1.93 (m, 1H), 1.22 (m, 40H), 0.87 (t, *J* = 6.5 Hz, 6H). ¹³C NMR (100 MHz, CDCl₃): δ 169.24, 139.38, 130.75, 128.66, 123.60, 122.44, 42.29, 37.33, 31.99, 31.66, 30.06, 29.72, 29.41, 26.48, 22.75, 14.18. MS (MALDI): *m/z* 596 (MH⁺). Anal. Calcd for C₃₆H₅₃NO₂S₂: C, 72.55; H, 8.96; N, 2.35. Found: C, 72.53; H, 8.90; N, 2.24%.

N-Dodecyl-2,7-dibromodithieno[3,2-f:2',3'-h]phthalimide (5a).

To a solution of **4a** (255 mg, 0.59 mmol) in 10 mL of CH_2Cl_2 was added Br₂ (382 mg, 2.39 mmol) and a small amount of FeCl₃ (5 mg). The mixture was allowed to stir in the dark for 4 h before 10 mL of saturated Na₂SO₃ aqueous solution was added. The organic layer was extracted by CH_2Cl_2 and dried over anhydrous MgSO₄. The crude product was purified by column chromatography on silica gel (CH_2Cl_2 /hexanes = 1:3) to give **5a** as a yellow solid (160 mg, 47%). ¹H NMR (400 MHz, CDCl₃): δ 8.03 (s, 2H), 3.70 (t, *J* = 7.2 Hz, 2H), 1.70 (m, 2H), 1.24 (m, 18H), 0.87 (t, *J* = 6.6 Hz, 3H). ¹³C NMR (100 MHz, CDCl₃): δ 167.92, 138.62, 130.41, 124.77, 122.36, 118.95, 38.17, 31.98, 29.69, 29.59, 29.41, 29.28, 29.17, 28.80, 26.98, 22.75, 14.20. HRMS (EI): 582.9843 (calcd for C₂₄H₂₇NO₂S₂Br₂, 582.9850). Anal. Calcd for C₂₄H₂₇NO₂S₂Br₂: C, 49.24; H, 4.65; N, 2.39. Found: C, 48.85; H, 4.61; N, 2.24%.

N-(2-Decyltetradecyl)-2,7-dibromodithieno[3,2-f:2',3'-h]phthalimide (5b).

The same procedure as **5a** using **4b** instead of **4a** to give **5b** as a yellow solid (40%). ¹H NMR (400 MHz, CDCl₃): δ 8.05 (s, 2H), 3.60 (d, *J* = 7.2 Hz, 2H), 1.89 (m, 1H), 1.22 (m, 40H), 0.89 (t, *J* = 6.7 Hz, 6H). ¹³C NMR (100 MHz, CDCl₃): δ 168.23, 138.76, 130.55, 124.91, 122.43, 118.91, 42.37, 37.29, 32.00, 31.63, 30.05, 29.74, 29.70, 29.44, 26.44, 22.77, 14.20. MS (MALDI): *m/z* 754 (MH⁺). Anal. Calcd for

$C_{36}H_{51}NO_2S_2Br_2$: C, 57.37; H, 6.82; N, 1.86. Found: C, 57.32; H, 6.90; N, 1.80%.

N-Dodecyl-2,7-bis(thiophen-2-yl)dithieno[3,2-f:2',3'-h]phthalimide (6a). To a solution of **5a** (163 mg, 0.28 mmol) and tributyl(thiophen-2-yl)stannane (224 mg, 0.6 mmol) in toluene (4 mL) was added $Pd(PPh_3)_4$ (23 mg, 0.02 mmol) under a N_2 atmosphere. After refluxing for 48 h, the mixture was cooled to room temperature and then poured into H_2O ; the organic layer was extracted by CH_2Cl_2 and dried over anhydrous $MgSO_4$. The crude product was purified by column chromatography on silica gel (CH_2Cl_2 /hexanes = 1:2) to give **6a** as a yellow solid (70 mg, 42%). 1H NMR (400 MHz, $CDCl_3$): δ 7.73 (s, 2H), 7.32 (d, J = 4.8 Hz, 2H), 7.21 (d, J = 2.9 Hz, 2H), 7.02 (d, J = 4.1 Hz, 2H), 3.61 (t, J = 7.1 Hz, 2H), 1.70 (m, 2H), 1.25 (m, 18H), 0.89 (t, J = 6.6 Hz, 3H). ^{13}C NMR (100 MHz, $CDCl_3$): δ 140.42, 137.29, 136.12, 131.68, 128.12, 126.84, 126.12, 122.97, 117.02, 116.97, 37.86, 31.98, 29.70, 29.62, 29.42, 29.32, 28.82, 27.03, 22.75, 14.19. HRMS (EI): 591.1390 (calcd for $C_{32}H_{33}NO_2S_4$, 591.1394). Anal. Calcd for $C_{32}H_{33}NO_2S_4$: C, 64.94; H, 5.62; N, 2.37. Found: C, 64.63; H, 5.61; N, 2.40%.

N-Dodecyl-2,7-bis(5-bromothiophen-2-yl)dithieno[3,2-f:2',3'-h]phthalimide (7a). To a solution of **6a** (70 mg, 0.12 mmol) in $CHCl_3$ / CH_3COOH (2 mL/2 mL) was added NBS (54 mg, 0.3 mmol) in one portion at 0 °C. After stirring overnight at room temperature and in dark, the mixture was poured into H_2O , and the organic layer was extracted by CH_2Cl_2 and dried over anhydrous $MgSO_4$. The crude product was purified by column chromatography on silica gel (CH_2Cl_2 /hexanes = 1:3) to give **7a** as a yellow solid (87 mg, 97%). 1H NMR (400 MHz, $CDCl_3$): δ 7.96 (s, 2H), 7.14 (d, J = 3.8 Hz, 2H), 7.07 (d, J = 3.8 Hz, 2H), 3.73 (t, J = 7.2 Hz, 2H), 1.74 (m, 2H), 1.24 (m, 18H), 0.88 (t, J = 6.0 Hz, 3H). MS (MALDI): m/z 747 (M^+). Anal. Calcd for $C_{32}H_{31}NO_2S_4Br_2$: C, 51.27; H, 4.17; N, 1.87. Found: C, 51.50; H, 4.32; N, 2.005%.

Poly[(4,8-didodecyloxybenzodithiophene-2,6-diyl)-alt-(N-decyldithieno[3,2-f:2',3'-h]phthalimide-2,7-diyl)] (P1). To a mixture of **5a** (88 mg, 0.15 mmol), 4,8-didodecyloxybenzodithiophene-2,6-ditin (132 mg, 0.15 mmol) in toluene (5 mL) was added $Pd(PPh_3)_4$ (20 mg, 0.015 mmol) under a N_2 atmosphere. The mixture was stirred at 110 °C for 3 days, and then 2-bromothiophene and tributyl(thiophen-2-yl)stannane were added subsequently to end-cap the polymer chain. After reaction mixture was cooled to room temperature, chloroform (100 mL) was added to the reaction mixture and washed with water. The organic layer was concentrated to 5 mL and dropped into methanol (200 mL). The precipitate was filtered. Finally, the polymer was purified by size exclusion column chromatography over Bio-Rad Biobeads S-X1 eluting with chloroform to afford a red solid (130 mg, 88%). 1H NMR (400 MHz, $CDCl_3$): δ 7.5 (br, 4H), 4.0 (br, 6H), 2.5–0.8 (br, 69H). Anal. Calcd for $(C_{58}H_{79}NO_4S_4)_n$: C, 70.90; H, 8.10; N, 1.43. Found: C, 69.32; H, 7.90; N, 1.20%. M_n , 12 250, M_w/M_n , 1.30.

Poly[(4,8-didodecyloxybenzodithiophene-2,6-diyl)-alt-(N-dodecyl-2,7-bis(thiophen-2-yl)dithieno[3,2-f:2',3'-h]phthalimide-5,5'-diyl)] (P2). To a mixture of **7a** (67 mg, 0.09 mmol), 4,8-didodecyloxybenzodithiophene-2,6-ditin (79 mg, 0.09 mmol) in toluene (4 mL) was added $Pd(PPh_3)_4$ (20 mg, 0.015 mmol) under a N_2 atmosphere. The mixture was stirred at 110 °C for 3 days, and then 2-bromothiophene and tributyl(thiophen-2-yl)stannane were added subsequently to end-cap the polymer chain. Reaction mixture was cooled to room temperature and dropped into methanol (200 mL). The precipitate was filtered to give a red solid (100 mg, 98%). We did not take any purification and measurements due to bad solubility in common organic solvents.

Poly[(4,4'-dihexyl-2,2'-bithiazole-5,5'-diyl)-alt-(N-decyldithieno[3,2-f:2',3'-h]phthalimide-2,7-diyl)] (P3). To a mixture of **5a** (129 mg, 0.22 mmol), 4,4'-dihexyl-2,2'-bithiazole-5,5'-ditin (146 mg, 0.22 mmol) in toluene (5 mL) was added $Pd(PPh_3)_4$ (20 mg, 0.015 mmol) under a N_2 atmosphere. The mixture was stirred at 110 °C for 3 days, and then 2-bromothiophene and tributyl(thiophen-2-yl)stannane were added subsequently to end-cap the polymer chain. Reaction mixture was

cooled to room temperature and dropped into methanol (200 mL). The precipitate was filtered to give a reddish-black solid (160 mg, 95%). We did not take any purification and measurements due to poor solubility in common organic solvents.

Poly[(4,4'-dihexyl-2,2'-bithiazole-5,5'-diyl)-alt-(N-(2-decyltetradecyl)dithieno[3,2-f:2',3'-h]phthalimide-2,7-diyl)] (P4). To a mixture of **5b** (150 mg, 0.2 mmol), 4,4'-dihexyl-2,2'-bithiazole-5,5'-ditin (133 mg, 0.2 mmol) in toluene (5 mL) was added $Pd(PPh_3)_4$ (20 mg, 0.015 mmol) under a N_2 atmosphere. The mixture was stirred at 110 °C for 3 days, and then 2-bromothiophene and tributyl(thiophen-2-yl)stannane were added subsequently to end-cap the polymer chain. After reaction mixture was cooled to room temperature, chloroform (100 mL) was added to the reaction mixture and washed with water. The organic layer was concentrated to 5 mL and dropped into methanol (200 mL). The precipitate was filtered. Finally, the polymer was purified by size exclusion column chromatography over Bio-Rad Biobeads S-X1 eluting with chloroform to afford a reddish-black solid (150 mg, 81%). 1H NMR (400 MHz, $CDCl_3$): δ 7.5 (br, 2H), 3.6 (br, 2H), 2.8 (br, 4H), 2.2–0.8 (br, 69H). Anal. Calcd for $(C_{54}H_{77}N_3O_2S_4)_n$: C, 69.85; H, 8.36; N, 4.53. Found: C, 67.58; H, 7.96; N, 4.023%. M_n , 9934, M_w/M_n , 1.43.

Poly[(benzothiadiazole-4,7-diyl)-alt-(N-(2-decyltetradecyl)dithieno[3,2-f:2',3'-h]phthalimide-2,7-diyl)] (P5). To a mixture of **5b** (132 mg, 0.175 mmol), 4,7-bis(4,4,5,5-tetramethyl-1,3,2-dioxaborolan-2-yl)benzo[*c*][1,2,5]thiadiazole (68 mg, 0.175 mmol) in toluene (10 mL) and 2 M K_2CO_3 aqueous solution (5 mL) was added $Pd(PPh_3)_4$ (20 mg, 0.015 mmol) under a N_2 atmosphere. The mixture was stirred at 110 °C for 3 days, and then 2-bromothiophene and 2-thiopheneboronic acid were added subsequently to end-cap the polymer chain. After reaction mixture was cooled to room temperature, chloroform (100 mL) was added to the reaction mixture and washed with water. The organic layer was concentrated to 5 mL and dropped into methanol (200 mL). The precipitate was filtered. Finally, the polymer was purified by size exclusion column chromatography over Bio-Rad Biobeads S-X1 eluting with chloroform to afford a black solid (97 mg, 76%). 1H NMR (400 MHz, $CDCl_3$): δ 7.8 (br, 4H), 3.6 (br, 2H), 2.4–0.8 (br, 47H). Anal. Calcd for $(C_{42}H_{53}N_3O_2S_3)_n$: C, 69.28; H, 7.34; N, 5.77. Found: C, 65.24; H, 7.05; N, 5.08%. M_n , 5714, M_w/M_n , 1.71.

Poly[N-(2-decyltetradecyl)dithieno[3,2-f:2',3'-h]phthalimide-2,7-diyl)] (P6). To a mixture of **5b** (75.4 mg, 0.1 mmol), hexabutyl-ditin (58 mg, 0.1 mmol) in toluene (5 mL) was added $Pd(PPh_3)_4$ (11 mg, 0.01 mmol) under a N_2 atmosphere. The mixture was stirred at 110 °C for 3 days, and then 2-bromothiophene and 2-thiopheneboronic acid were added subsequently to end-cap the polymer chain. After reaction mixture was cooled to room temperature, chloroform (100 mL) was added to the reaction mixture and washed with water. The organic layer was concentrated to 5 mL and dropped into methanol (200 mL). The precipitate was filtered. Finally, the polymer was purified by size exclusion column chromatography over Bio-Rad Biobeads S-X1 eluting with chloroform to afford a black solid (70 mg, 93%). 1H NMR (400 MHz, $CDCl_3$): δ 7.9 (br, 2H), 3.7 (br, 2H), 2.4–1.2 (br, 41H), 0.9 (br, 6H). Anal. Calcd for $(C_{36}H_{51}NO_2S_2)_n$: C, 72.55; H, 8.96; N, 2.35. Found: C, 70.24; H, 8.75; N, 2.08%. M_n , 10 053, M_w/M_n , 1.56.

■ ASSOCIATED CONTENT

S Supporting Information. Absorption and emission spectra of compound **4b** in chloroform solution and in film; 1H NMR spectra of **5a,b**, **7a**, **P1**, and **P4–P6**. This material is available free of charge via the Internet at <http://pubs.acs.org>.

■ AUTHOR INFORMATION

Corresponding Author

*E-mail: xwzhan@iccas.ac.cn.

■ ACKNOWLEDGMENT

This work was supported by NSFC (Grants 21025418, 50873107, and 21021091), 973 Project (Grant 2011CB808401), and the Chinese Academy of Sciences.

■ REFERENCES

- (1) Heeger, A. J. *Angew. Chem., Int. Ed.* **2001**, *40*, 2591.
- (2) Zhao, X. G.; Zhan, X. W. *Chem. Soc. Rev.* **2011**, *40*, 1039/COCS00194E.
- (3) Anthony, J. E.; Facchetti, A.; Heeney, M.; Marder, S. R.; Zhan, X. W. *Adv. Mater.* **2010**, *22*, 3876.
- (4) Zhan, X. W.; Facchetti, A.; Barlow, S.; Marks, T. J.; Ratner, M. A.; Wasielewski, M. R.; Marder, S. R. *Adv. Mater.* **2011**, *23*, 268.
- (5) Zhan, X. W.; Tan, Z. A.; Domercq, B.; An, Z. S.; Zhang, X.; Barlow, S.; Li, Y. F.; Zhu, D. B.; Kippelen, B.; Marder, S. R. *J. Am. Chem. Soc.* **2007**, *129*, 7246.
- (6) Zhang, L.; Di, C. A.; Zhao, Y.; Guo, Y. L.; Sun, X. N.; Wen, Y. G.; Zhou, W. Y.; Zhan, X. W.; Yu, G.; Liu, Y. Q. *Adv. Mater.* **2010**, *22*, 3537.
- (7) Tan, Z. A.; Zhou, E. J.; Zhan, X. W.; Wang, X.; Li, Y. F.; Barlow, S.; Marder, S. R. *Appl. Phys. Lett.* **2008**, *93*, 073309.
- (8) Zhan, X. W.; Tan, Z. A.; Zhou, E. J.; Li, Y. F.; Misra, R.; Grant, A.; Domercq, B.; Zhang, X. H.; An, Z. S.; Zhang, X.; Barlow, S.; Kippelen, B.; Marder, S. R. *J. Mater. Chem.* **2009**, *19*, 5794.
- (9) Zhan, X. W.; Zhu, D. B. *Polym. Chem.* **2010**, *1*, 409.
- (10) Chen, Z. H.; Zheng, Y.; Yan, H.; Facchetti, A. *J. Am. Chem. Soc.* **2009**, *131*, 8.
- (11) Yan, H.; Chen, Z. H.; Zheng, Y.; Newman, C.; Quinn, J. R.; Dotz, F.; Kastler, M.; Facchetti, A. *Nature* **2009**, *457*, 679.
- (12) Witzel, S.; Ott, C.; Klemm, E. *Macromol. Rapid Commun.* **2005**, *26*, 889.
- (13) Dierschke, F.; Jacob, J.; Muellen, K. *Synth. Met.* **2006**, *156*, 433.
- (14) Guo, X. G.; Kim, F. S.; Jenekhe, S. A.; Watson, M. D. *J. Am. Chem. Soc.* **2009**, *131*, 7206.
- (15) Zhang, Q. T.; Tour, J. M. *J. Am. Chem. Soc.* **1997**, *119*, 5065.
- (16) Zhang, Q. T.; Tour, J. M. *J. Am. Chem. Soc.* **1998**, *120*, 5355.
- (17) Pomerantz, M. *Synth. Met.* **2003**, *135–136*, 257.
- (18) Pomerantz, M. *Tetrahedron Lett.* **2003**, *44*, 1563.
- (19) Nielsen, C.; Bjornholm, T. *Org. Lett.* **2004**, *6*, 3381.
- (20) Zhang, G.; Fu, Y.; Zhang, Q.; Xie, Z. *Chem. Commun.* **2010**, *46*, 4997.
- (21) Zou, Y.; Najari, A.; Berrouard, P.; Beaupré, S.; Aïch, B. R.; Tao, Y.; Leclerc, M. *J. Am. Chem. Soc.* **2010**, *132*, 5330.
- (22) Piliago, C.; Holcombe, T. W.; Douglas, J. D.; Woo, C. H.; Beaujuge, P. M.; Fréchet, J. M. J. *J. Am. Chem. Soc.* **2010**, *132*, 7579.
- (23) Zhang, Y.; Hau, S. K.; Yip, H.-L.; Sun, Y.; Acton, O.; Jen, A. K. Y. *Chem. Mater.* **2010**, *22*, 2696.
- (24) Guo, X. G.; Xin, H.; Kim, F. S.; Liyanage, A. D. T.; Jenekhe, S. A.; Watson, M. D. *Macromolecules* **2011**, *44*, 269.
- (25) Meng, H.; Wudl, F. *Macromolecules* **2001**, *34*, 1810.
- (26) Sonmez, G.; Meng, H.; Wudl, F. *Chem. Mater.* **2003**, *15*, 4923.
- (27) Letizia, J. A.; Salata, M. R.; Tribout, C. M.; Facchetti, A.; Ratner, M. A.; Marks, T. J. *J. Am. Chem. Soc.* **2008**, *130*, 9679.
- (28) Xiao, K.; Liu, Y. Q.; Qi, T.; Zhang, W.; Wang, F.; Gao, J. H.; Qiu, W. F.; Ma, Y. Q.; Cui, G. L.; Chen, S. Y.; Zhan, X. W.; Yu, G.; Qin, J. G.; Hu, W. P.; Zhu, D. B. *J. Am. Chem. Soc.* **2005**, *127*, 13281.
- (29) Zhang, S. M.; Guo, Y. L.; Zhang, Y. J.; Liu, R. G.; Li, Q. K.; Zhan, X. W.; Liu, Y. Q.; Hu, W. P. *Chem. Commun.* **2010**, *46*, 2841.
- (30) Wu, W. P.; Liu, Y. Q.; Zhu, D. B. *Chem. Soc. Rev.* **2010**, *39*, 1489.
- (31) Liu, Y.; Liu, Y. Q.; Zhan, X. W. *Macromol. Chem. Phys.* **2011**, *212*, 428.
- (32) Huang, X. B.; Zhu, C. L.; Zhang, S. M.; Li, W. W.; Guo, Y. L.; Zhan, X. W.; Liu, Y. Q.; Bo, Z. S. *Macromolecules* **2008**, *41*, 6895.
- (33) Huang, X. B.; Shi, Q. Q.; Chen, W. Q.; Zhu, C. L.; Zhou, W. Y.; Zhao, Z.; Duan, X. M.; Zhan, X. W. *Macromolecules* **2010**, *43*, 9620.
- (34) Yamaguchi, S.; Swager, T. M. *J. Am. Chem. Soc.* **2001**, *123*, 12087.
- (35) Song, C.; Swager, T. M. *J. Org. Chem.* **2010**, *75*, 999.
- (36) Rieger, R.; Beckmann, D.; Pisula, W.; Steffen, W.; Kastler, M.; Müllen, K. *Adv. Mater.* **2010**, *22*, 83.
- (37) Xiao, S.; Zhou, H.; You, W. *Macromolecules* **2008**, *41*, 5688.
- (38) Xiao, S.; Andrew, C. S.; Liu, S.; You, W. *ACS Appl. Mater. Interfaces* **2009**, *1*, 1613.
- (39) Zhou, H.; Yang, L.; Stoneking, S.; You, W. *ACS Appl. Mater. Interfaces* **2010**, *2*, 1377.
- (40) Zhou, H.; Yang, L.; Xiao, S.; Liu, S.; You, W. *Macromolecules* **2010**, *43*, 811.
- (41) Dubernet, M.; Caubert, V.; Guillard, J.; Viaud-Massuard, M.-C. *Tetrahedron* **2005**, *61*, 4585.
- (42) Tovar, J. D.; Rose, A.; Swager, T. M. *J. Am. Chem. Soc.* **2002**, *124*, 7762.
- (43) Wang, H. F.; Wen, Y. G.; Yang, X. D.; Wang, Y.; Zhou, W. Y.; Zhang, S. M.; Zhan, X. W.; Liu, Y. Q.; Shuai, Z. G.; Zhu, D. B. *ACS Appl. Mater. Interfaces* **2009**, *1*, 1122.
- (44) Jia, M.; Ma, X.; Yan, L.; Wang, H.; Guo, Q.; Wang, X.; Wang, Y.; Zhan, X.; Xia, A. *J. Phys. Chem. A* **2010**, *114*, 7345.
- (45) Zaumseil, J.; Sirringhaus, H. *Chem. Rev.* **2007**, *107*, 1296.
- (46) Newman, C. R.; Frisbie, C. D.; da Silva Filho, D. A.; Brédas, J.-L.; Ewbank, P. C.; Mann, K. R. *Chem. Mater.* **2004**, *16*, 4436.
- (47) Shi, Q. Q.; Fan, H. J.; Liu, Y.; Hu, W. P.; Li, Y. F.; Zhan, X. W. *J. Phys. Chem. C* **2010**, *114*, 16843.